

# Polymer Blends Spin-Cast into Films with Complementary Elements for Electronics and Biotechnology

Andrzej Budkowski,<sup>1</sup> Joanna Zemła,<sup>1</sup> Ellen Moons,<sup>2</sup> Kamil Awsiuk,<sup>1</sup> Jakub Rysz,<sup>1</sup> Andrzej Bernasik,<sup>3</sup> Cecilia M. Björström-Svanström,<sup>2</sup> Małgorzata Lekka,<sup>4</sup> Justyna Jaczewska<sup>1</sup>

<sup>1</sup>Smoluchowski Institute of Physics, Jagiellonian University, Kraków, Poland

<sup>2</sup>Department of Physics and Electrical Engineering, Karlstad University, Karlstad, Sweden

<sup>3</sup>Faculty of Physics and Applied Computer Science, AGH - University of Science and Technology, Kraków, Poland

<sup>4</sup>Niewodniczanski Institute of Nuclear Physics, Polish Academy of Science, Kraków, Poland

Received 30 November 2011; accepted 30 November 2011

DOI 10.1002/app.36574

Published online in Wiley Online Library (wileyonlinelibrary.com).

**ABSTRACT:** Versatility of solution-processing strategy based on the simultaneous rather than additive deposition of different functional molecules is discussed. It is shown that spin-cast polymer blends result in films with domains that could form elements with complementary functions of (i) solar cells, (ii) electronic circuitries, and (iii) test plates for protein micro-arrays: Alternating layers, rich in electron-donating polyfluorene and electron-accepting fullerene derivative, result in optimized solar power conversion. Surface patterns, made by soft lithography, align conductive paths of conjugated poly(3-alkylthiophene) in dielectric polystyrene. Proteins, preserving their biological activity, are adsorbed to hydrophobic domains of polystyrene in hydrophilic matrix of poly(ethylene oxide). The authors report the research progress on structure formation in three polymer blend families,

resulting in films with complementary elements for electronics and biotechnology. Blend film structures are determined with secondary ion mass spectrometry, atomic force microscopy, and fluorescence microscopy. In addition, the authors present recent results on (i) structure formation in fullerene derivative/poly(3-alkylthiophene) blends intended for solar cells, (ii) 3-dimensional SIMS imaging of conductive paths of poly(3-alkylthiophene) in dielectric polystyrene, (iii) test plates for multiprotein micro-arrays fabricated with blend films of hydrophobic polystyrene and thermoresponsive poly(*N*-isopropylacrylamide). © 2012 Wiley Periodicals, Inc. *J Appl Polym Sci* 000: 000–000, 2012

**Key words:** spin coating; thin blend films; self-assembly; conjugated polymers; biological applications of polymers

## INTRODUCTION

In contrast to classical materials, metals or semiconductors, functional organic macromolecules can be dissolved in solvent and retrieved after solvent evaporation as deposited solid films. In the past decade, solution processing has been applied in numerous low-cost fabrication methods proposed for electronics<sup>1–7</sup> and biotechnology.<sup>8–11</sup> Spin-coating,<sup>12</sup> as the first deposition technique, has been successfully implemented on manufacturing lines.<sup>2</sup> Mainstream strategies following this approach are based on *additive* deposition of different molecules (e.g., with screen-,<sup>13</sup> inkjet-,<sup>7</sup> and micro-contact-<sup>14</sup> printing) to fabricate *step-by-step* all the components of the prototype devices.

Spin-coating of the dissolved polymer blends is technologically more attractive than successive molecular deposition procedures: it offers a *one-step* process, in which phase domains rich in different

blend components are formed and self-assemble spontaneously, constituting the various device elements.<sup>15–19</sup> To demonstrate the versatility of this *one-step* deposition approach, the authors show in this article that spin-cast polymer blends can result in film domains that could form complementary elements of (a) solar cells, (b) electronic circuitries, and (c) test plates for protein micro-arrays. The binary mixtures used consisting of pairs of molecules with complementary functionality (Fig. 1): (a) electron-donating and hole-transporting polyfluorene and electron-accepting fullerene derivative,<sup>20,23–26</sup> (b) conjugated poly(3-alkylthiophene) and dielectric polystyrene,<sup>21,27–29</sup> (c) hydrophobic polystyrene and hydrophilic poly(ethylene oxide).<sup>22,30</sup> In addition, the specific structures intended for these different applications result from differences in the dominant phase separation processes,<sup>31</sup> such as self-stratification [Fig. 1(a)],<sup>23,32–34</sup> domain alignment by surface pattern [Fig. 1(b)],<sup>21,35,36</sup> and partial surface wetting by blend phases [Fig. 1(c)].<sup>22,29,37</sup> These processes are closely related with each other. For instance, depending on spin-casting parameters, self-stratified lamellar structures can be “broken up” due to interfacial instabilities<sup>27,29,38</sup> into lateral (quasi-2-dim) domains partially wetting the surface. Therefore, it

Correspondence to: A. Budkowski (ufbudkow@cyf-kr.edu.pl).

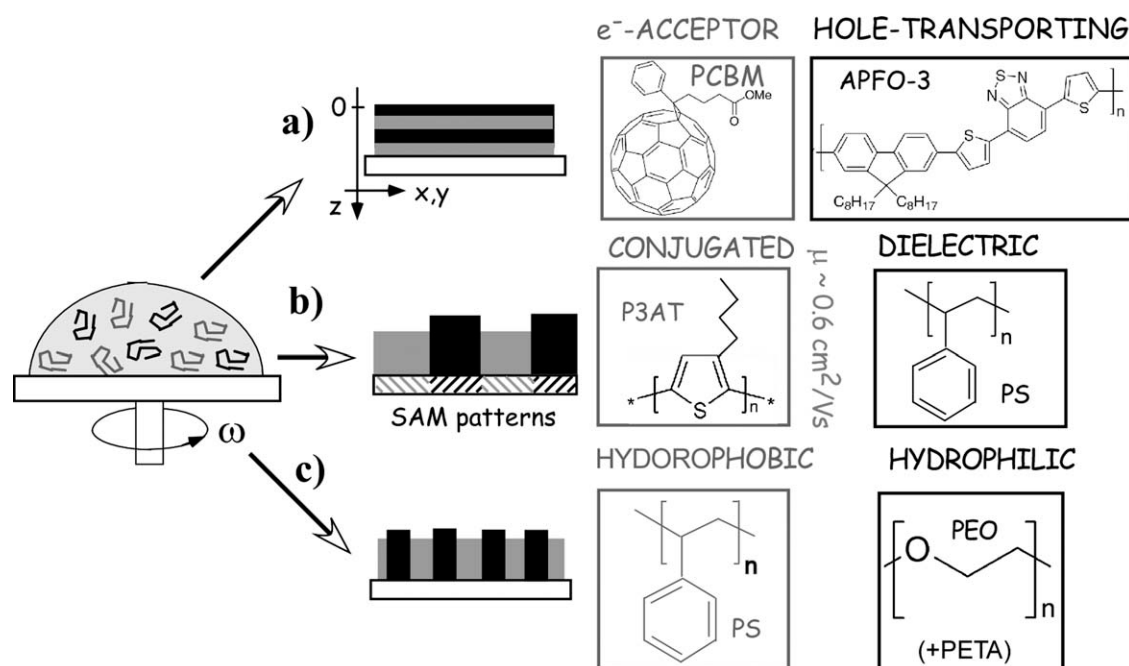


**Figure 1** Film structures with domains that form elements with complementary functions of (a) solar cells, (b) electronic circuitries, and (c) test plates for protein micro-arrays, obtained when spin-cast are binary mixtures of molecules with complementary functionality: (a) electron-donating polyfluorene copolymer APFO-3 and electron-accepting fullerene derivative PCBM, (b) conjugated poly(3-alkylthiophene) P3AT and dielectric polystyrene PS, (c) hydrophobic polystyrene PS and hydrophilic poly(ethylene oxide) PEO (with admixed cross-linking agent pentaerythritol triacrylate, PETA).

is instructive to discuss the physical origins of self-stratification, illustrated for fullerene derivative blends in solar cells, prior to the stability analysis of lamellar and lateral structures, relevant for the phase rearrangement of poly(3-alkylthiophene) blends spin-cast for polymer circuitries. In this article, the authors report progress in the research on structure formation in three polymer blend families (Fig. 1), resulting in films with complementary elements for electronics and biotechnology. Moreover, the authors present recent developments on (a) structure formation in fullerene derivative/poly(3-alkylthiophene) blends intended for solar cells, (b) 3-dimensional imaging of conductive paths of poly(3-alkylthiophene) in dielectric polystyrene, (c) test plates for multiprotein micro-arrays fabricated with blend films of hydrophobic polystyrene and thermoresponsive poly(*N*-isopropylacrylamide).

## EXPERIMENTAL

### Polymer sample preparation

APFO-3 (poly[(9,9-dioctylfluorenyl-2,7-diyl)-alt-5,5-(40,70-di-2-thienyl-20,10,30-benzothiadiazole)]): d5-PCBM (pentadeuterated form of [6,6]-phenyl- $C_{61}$ -butyric acid methyl ester) blend solutions (blend ratio 1 : 1 and 1 : 4 by weight) were prepared in chloroform with a total concentration of solids  $C_s = 12$  mg/mL. R-P3HT [regio-regular poly(3-hexylthiophene)]: d5-PCBM blend solutions (blend ratio 1 : 4 by weight) were prepared

in chloroform with concentration  $C_s = 15$  mg/mL. Thin films were spin-coated onto silicon wafers or PEDOT:PSS layers cast on glass covered with indium tin oxide (ITO).

Solutions of R-P3HT, poly(3-dodecylthiophene) P3DDT, and polystyrene PS (blend ratio 1 : 1 by weight) were diluted in chloroform with concentration  $C_s = 20$  mg/mL. Polymer solutions were spin-cast with various spinning speeds  $\omega$ , adjusted carefully to obtain the best possible pattern transposition into the blend morphology, for 30 s on silicon wafer modified earlier by micro-contact printing with self-assembled monolayers (SAM) of octadecyltrichlorosilane.

To prepare PS/poly(methyl methacrylate) (PMMA), PS/poly(ethylene oxide) (PEO), and PS/poly(*N*-isopropylacrylamide) (PNIPAM) films, their binary blends in toluene (PS/PMMA), or chloroform (PS/PEO and PS/PNIPAM) were used. The solutions of PEO and PNIPAM blends were admixed with small amount of cross-linking agent.<sup>30</sup> The PS/PMMA blend films were used as cast, while the PS/PEO and PS/PNIPAM films were additionally cross-linked with ultraviolet radiation (high pressure Hg lamp, 400 W, for 2 h) to prevent from polymer dissolution during subsequent protein deposition.<sup>30</sup>

### Protein adsorption

To test protein adsorption, two lectins (Biokom, Poland) were used: concanavalin A from *Canavalia ensiformis* (Con A) and lentil lectin from *Lens*

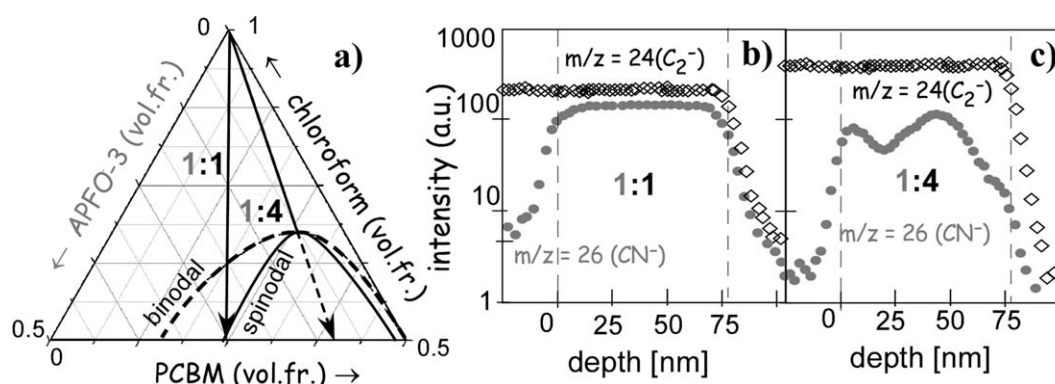


**Figure 2** Spin-casting of APFO-3:PCBM mixtures with blend weight ratios 1 : 4 and 1 : 1, dissolved in chloroform, results in different quench paths marked with arrows in the phase diagram of the ternary APFO-3:PCBM:chloroform system (a) and in different final film structures revealed by SIMS<sup>23</sup> as depth profiles of APFO-3 composition ( $m/z = 26$ ) and organic ( $m/z = 24$ ) signal (b,c).

*culinaris* (LcH). Both lectins were fluorescently labeled, ConA with the fluorescein isothiocyanate (FITC), absorbing blue light ( $\lambda_{\text{abs}} = 490$  nm) and emitting green fluorescence ( $\lambda_{\text{emit}} = 525$  nm) and LcH with tetramethylrhodamine isothiocyanate (TRICT), absorbing green light ( $\lambda_{\text{abs}} = 557$  nm) and emitting red fluorescence ( $\lambda_{\text{emit}} = 576$  nm). The solutions of proteins in phosphate buffer saline (PBS, pH 7.4, Sigma) were prepared, with concentration  $c = 125$   $\mu\text{g}/\text{mL}$ . The drop of each solution was placed on the patterned polymer substrate at  $24^\circ\text{C}$  for incubation time  $t = 15$  min, then the sample was rinsed carefully with PBS and placed in PBS buffer. For PS/PNIPAM blend, this procedure was applied once more at temperature of  $38^\circ\text{C}$ . To verify the biological activity of proteins adsorbed to polymer patterns, the experiment on recognition between a glycoprotein carboxypeptidase Y (CaY, Sigma) and a lectin Con A was performed.<sup>22</sup>

### Characterization

Phase structure of polymer blend surfaces was examined with Atomic Force Microscopy (AFM Agilent 5500, The Academia System from Nanonics Imaging, Israel) working in noncontact and contact modes. Fluorescence microscopy was performed with Olympus Reflected Fluorescence System. The samples with immobilized proteins were immersed in PBS buffer.

Dynamic secondary ion mass spectrometry technique was used to investigate composition within thin films. Composition versus depth profiles were obtained by a VSW system equipped with gallium liquid metal ion gun (FEI company) and quadrupole mass spectrometer (Balzers). Primary  $\text{Ga}^+$  beam (5 keV, 2 nA) was rastered over  $100 \mu\text{m} \times 100 \mu\text{m}$  area and secondary ions emerging from the central part (50%) of the sputtered crater were analyzed in the mass spectrometer. Each sample was covered with

thin layer of polystyrene, prior to SIMS experiment to reach steady state of the sputtering process before the investigated film was exposed. Three dimensional distribution of thin film components were obtained by a time-of-flight SIMS apparatus (TOF-SIMS 5, ION-TOF GmbH) working in dual beam mode. Samples were sputtered by low energy  $\text{Cs}^+$  ion beam (500 eV, 35 nA), rastered over  $500 \mu\text{m} \times 500 \mu\text{m}$  area, and revealed this way internal structures of thin films were analyzed with  $\text{Bi}^+$  30 keV pulsed ion beam ( $50 \mu\text{m} \times 50 \mu\text{m}$  central region only).

### Multilayers for organic solar cells

The first mixture, intended for solar cells, consists of conjugated polyfluorene copolymer APFO3 (poly[(9,9-dioctylfluorenyl-2,7-diyl)-alt-5,5-(40,70-di-2-thienyl-20,10,30-benzothiadiazole)]) and a fullerene derivative, PCBM ([6,6]-phenyl- $\text{C}_{61}$ -butyric acid methyl ester).<sup>20,23–26</sup> This blend dissolved in chloroform was used to spin-cast films, which were analyzed with secondary ion mass spectrometry to determine how their composition varies with depth. SIMS data reveal that composition waves are formed readily during spin-casting [cf. Fig. 2(c) and Fig. 2(b)] when the blend composition (1 : 4 rather than 1 : 1 APFO-3:PCBM blend weight ratio) allows for an easy access to the unstable (spinodal) region of the phase diagram [solid line curve in Fig. 2(a)], with the quench (marked by arrows) enabled by solvent extraction from an initially three-component film.<sup>24,26</sup> This indicates spontaneous spinodal phase separation, driven, and ordered by surface segregation (for APFO-3 and PCBM at free surface and substrate, respectively), as the mechanism responsible for self-stratification,<sup>32–34</sup> i.e., the self-assembly of de-mixed blend domains into a lamellar structure.

Because APFO-3 is an electron-donating and hole-transporting polymer (with lower ionization



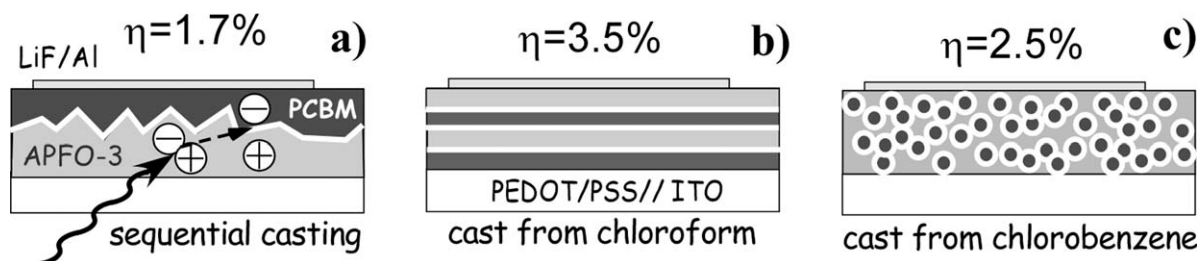


**Figure 3** Photo-generated electron-hole pairs (excitons) dissociate at heterojunctions formed in APFO-3/PCBM films. Various films structures: diffuse bilayer (a), self-stratified multilayer (b), and homogeneous blend morphology (c), result in different efficiencies  $\eta$  of solar power conversion.<sup>20</sup>

potential), and PCBM is an electron-accepting molecule (with higher electron affinity), donor/acceptor interfaces (heterojunctions) are formed readily in the spin-cast films composed of APFO-3 and PCBM. Electron-hole pairs (excitons) created by light can dissociate efficiently into free charges at the donor/acceptor interfaces, and therefore, heterojunctions are important for solar cells.<sup>39–41</sup> In addition, because exciton diffusion length is limited to c.a. 10 nm (for conjugated polymers)<sup>42</sup> all excitons created (in APFO-3) further away from the narrow regions near the heterojunctions are lost for the charge generation. Charge separation but also charge transport is affected by the film structure of the domains rich in donor and acceptor.

Three types of the PCBM/APFO-3 film structures were analyzed. Their structures, determined rigorously with SIMS,<sup>20</sup> are presented schematically in Figure 3. Diffuse bilayer was obtained by sequential casting from different solvents (APFO-3 from chloroform, PCBM from dichloromethane). Extended interfaces between APFO-3 and PCBM lamellae were detected when the APFO-3:PCBM mixture (with 1 : 4 blend ratio) was spin-cast from chloroform resulting in self-stratified multilayer, as described earlier. In turn, homogeneous blend morphology due to PCBM aggregates dispersed in the APFO-3 matrix was concluded when the same APFO-3:PCBM mixture was spin-cast from chlorobenzene. The solvent exchange for the less volatile chlorobenzene enables the slow nucleation of PCBM nanocrystals to compete kinetically with surface-directed liquid-liquid phase separation.<sup>26</sup> Solar cells with all three types of the PCBM/APFO-3 film structures are significantly affected by film morphology, resulting in different efficiencies  $\eta$  of solar power conversion<sup>20</sup> (Fig. 3). The interfacial area between donor and acceptor is larger for spin-cast blends when compared with the sequentially cast bilayer [Fig. 3(a)], resulting in increased charge generation and hence in higher  $\eta$  values. In addition, the self-stratified multilayer [Fig. 3(b)] promotes the generation and separation of charge carriers more effectively than the film with homogeneously dis-

persed PCBM nanocrystals [Fig. 3(c)] (resembling leaky diode).

The above results, presented for the fullerene/polyfluorene blends, suggest self-stratification of spin-cast blend films, favored by fast evaporation of chloroform, as the promising strategy for solar cell fabrication. However, this multilayer formation strategy fails when polyfluorene APFO-3 is exchanged with regio-regular poly(3-hexylthiophene) R-P3HT as a blend component. No composition waves are visible in SIMS depth profiles [Fig. 4(b)], indicating vertically homogeneous structure. This reflects early stage of spinodal phase separation that is not ordered by external surfaces [Fig. 4(a)]. The reason for this is smaller difference in surface energy between fullerene and polymer as well as smaller strength of polymer/fullerene interaction parameter governing interfacial energy.<sup>26,41,43</sup> Resulting structure of R-P3HT/PCBM films, forming so-called bulk heterojunction, is the subject of intensive research.<sup>41</sup>

### Structures for polymer circuitries

One of the most studied conjugated polymer families are poly(3-alkylthiophenes) P3ATs. This is due to their superior charge mobility and commercial availability.<sup>44</sup> Polythiophene blends with dielectric polymers have been spin-cast to form films with *lamellar* (L) or *lateral*, i.e., *quasi-2-dim* (2) structures [see Fig. 5(b)], used to fabricate prototypes of field-effect transistors<sup>45,46</sup> and light-emitting diodes,<sup>47,48</sup> respectively.

Film morphology formation in spin-cast P3AT blends involves self-stratification of lamellar structure L (with P3AT-rich lamella covered by layer rich in dielectric polymer). The lamellar structure (L) can be either frozen in or be unstable (due to Marangoni-like instability of polymer/polymer interface) resulting in lateral, quasi-2-dim morphology (2).<sup>27,29,38</sup>

One could control the morphology of polymer blend films using the concept of surface phase transition<sup>37</sup> from *partial wetting*—with two blend phases facing the substrate—to *complete wetting*—with only one polymer phase at the surface [Fig. 5(a,b)]. This

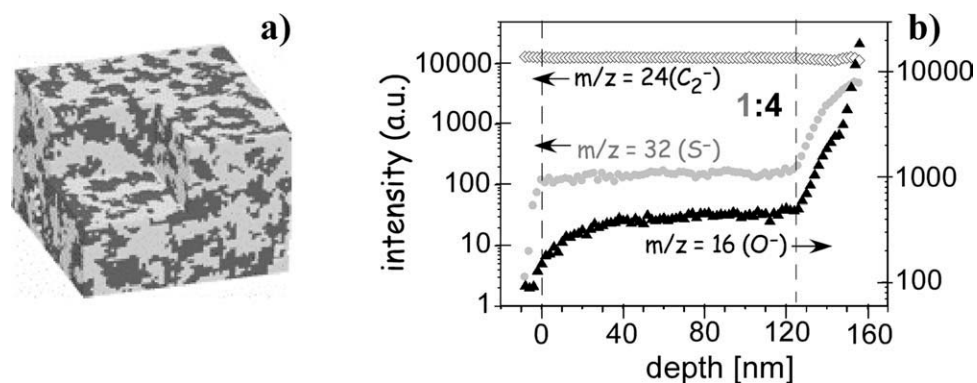


**Figure 4** Spin-coating onto PEDOT:PSS covered indium tin oxide ITO the mixtures R-P3HT:PCBM with blend weight ratio 1 : 4, dissolved in chloroform, results in vertically homogeneous film structure (a), revealed by SIMS (b) as depth profiles of R-P3HT composition ( $m/z = 32$ , left scale), organic ( $m/z = 24$ , left scale), and oxygen ( $m/z = 16$ , right scale) signal (cf. Fig. 2c for the mixture APFO-3:PCBM).

transition, observed originally for annealed blends (due to temperature quench),<sup>49</sup> can be of relevance also for spin-cast P3AT:PS blends (solvent quench).<sup>29</sup> It is induced by a changed relation between work of adhesion and work of cohesion (Fig. 5). Therefore, morphological control on spin-cast blend films is

possible, when blend component (i.e., work of cohesion)<sup>29</sup> or substrate (i.e., work of adhesion)<sup>21</sup> is changed. For instance, the exchange of poly(3-dodecylthiophene) P3DDT for its regio-regular counterpart R-P3DDT as a component in the P3AT:PS blend spin-cast on silicon oxide  $\text{SiO}_x$  (from various

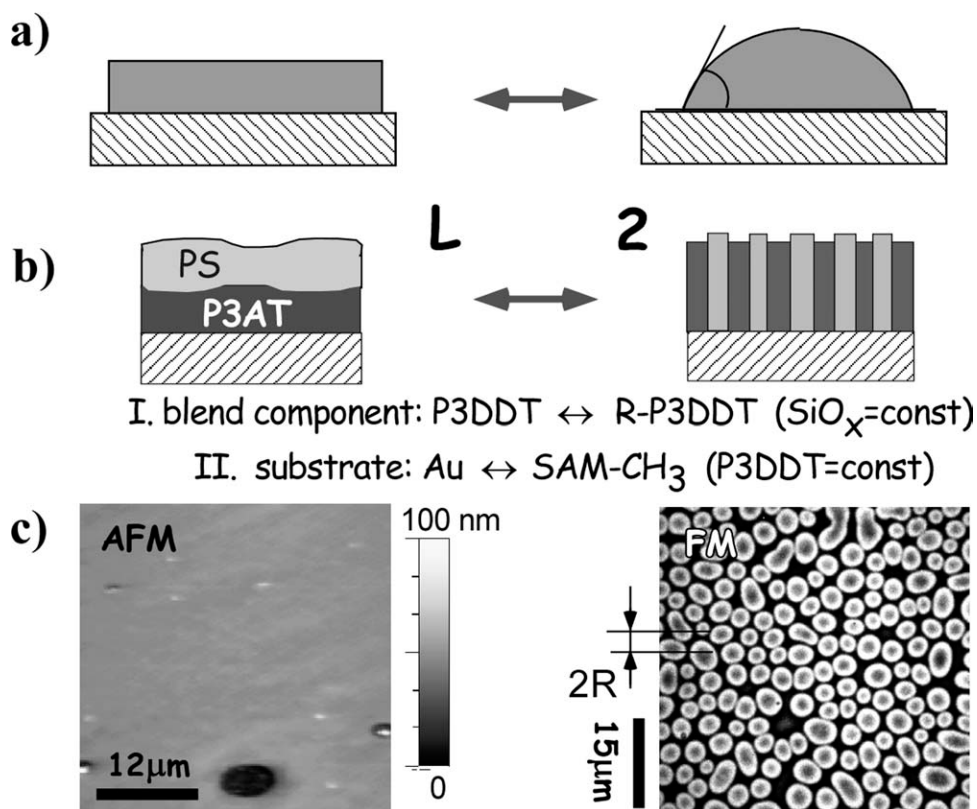


**Figure 5** Spin-cast P3AT blends with dielectric polymers (PS). The final blend film morphology is dependent on the relation between work of adhesion  $W_{\text{adh}}$  and work of cohesion  $W_{\text{coh}}$  of the blend phases. In analogy to a surface phase transition (a) from complete ( $W_{\text{adh}} \geq W_{\text{coh}}$ , left) to partial wetting ( $W_{\text{adh}} < W_{\text{coh}}$ , right), the spin-cast P3AT:PS blends will result in lamellar (L) or quasi-2-dim lateral (2) structures (b). In practice, a morphological transition can be induced in P3AT/PS films when blend component ( $W_{\text{coh}}$ ) or substrate ( $W_{\text{adh}}$ ) is varied. The latter is demonstrated with AFM (left) and fluorescence (right) micrographs (c) recorded for P3DDT/PS blends cast on gold, bare (left), and covered with hexadecanethiol (right).<sup>21</sup>

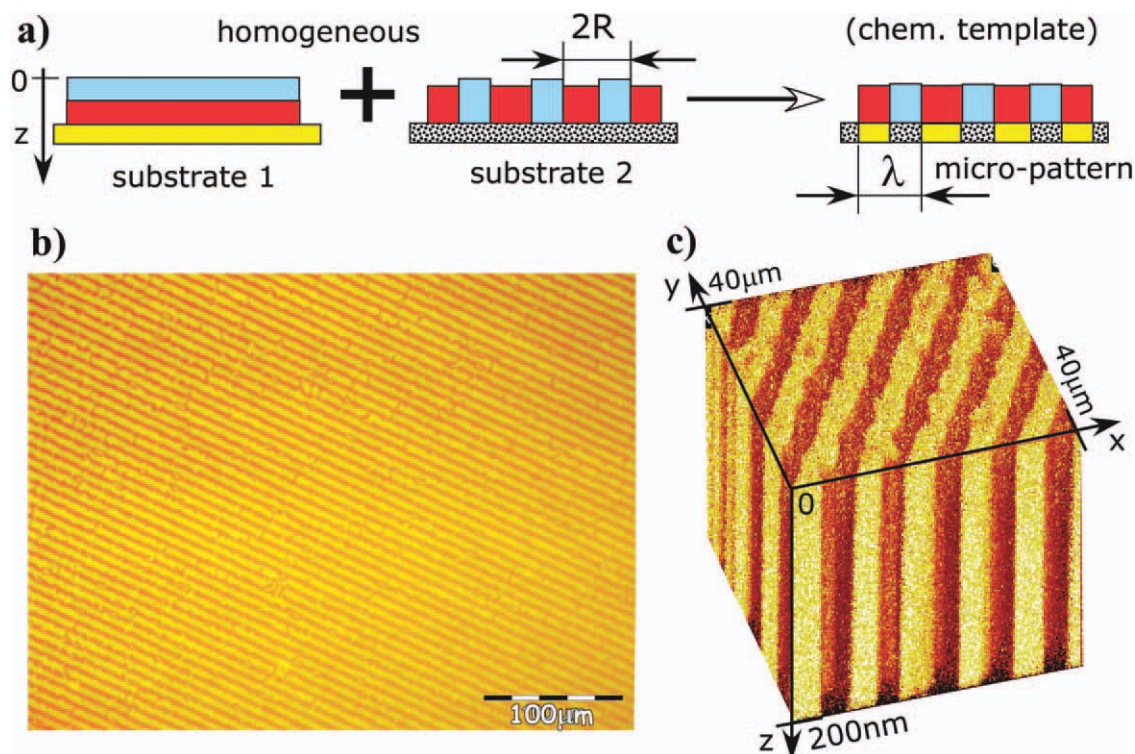


**Figure 6** (a) A substrate completely wetted by one of blend phases can be used to construct micro-patterns (with periodicity  $\lambda$ ) that align the blend domains (with inherent domain scale  $2R$ ). Nearly ideal alignment, obtained for  $\lambda$  matching  $2R$  (the latter adjusted by the spinning speed), is demonstrated for a R-P3HT:PS blend spin-cast on a  $\text{SiO}_x$  substrate patterned with SAM: (b) Fluorescent micrograph of R-P3HT domains aligned over large areas in this R-P3HT:PS blend thin film. (c) 3-dim distribution of R-P3HT obtained from SIMS ( $\text{S}^-$  and  $\text{SH}^-$  ions,  $m/z = 32$  and  $33$ ), with the lateral structure extending throughout the blend film. [Color figure can be viewed in the online issue, which is available at [wileyonlinelibrary.com](http://wileyonlinelibrary.com).]

solvents) induces a transition from lamellar to quasi-2-dim film morphology.<sup>29</sup> In turn, the strong adhesion between P3DDT and the gold substrate (due to specific thiophene–Au interactions), driving lamellar structure [see AFM image in Fig. 5(c)], can be blocked by the use of SAM of hexadecanethiol, resulting in a lateral morphology with fluorescent polythiophene domains visible in fluorescence micrographs [Fig. 5(c)].

The question arises whether surfaces micro-patterned with both substrate types, i.e., the ones resulting in macroscopic lamellar and lateral (quasi-2-dim) structures when used independently, can provide a chemical template for ordering *laterally* arranged domains of spin-cast blends<sup>35,36</sup> of conjugated polythiophenes and a dielectric polymer [Fig. 6(a)]. Previous studies have shown that SAM templates generated locally with dip-pen nanolithography<sup>50,51</sup> or macroscopically with digital lithography,<sup>52</sup> induce laterally controlled *lamellar* phase structure of spin-cast PS mixtures with poly(3-hexylthiophene) P3HT and poly(methyl methacrylate) blends with poly[5,5'-bis(3-dodecyl-2-thienyl)-2,2'-bithiophene], respectively. The problem is resolved in our more recent work,<sup>21</sup> showing that the domain structures of spin-cast P3AT/PS blends can be aligned with

chemical micro-patterns (SAM/Au, SAM/ $\text{SiO}_x$ , Au/ $\text{SiO}_x$ ) prepared by soft- or photo-lithography on silicon wafers (covered with  $\text{SiO}_x$  or Au).<sup>21</sup> This approach is illustrated in this article with the film morphology of regio-regular P3HT blended with PS and spin-cast from chloroform onto a silicon wafer, micro-contact printed with a SAM of octadecyltrichlorosilane. The fluorescent image [Fig. 6(b)] shows nearly perfect pattern-directed alignment of the R-P3HT domains with the substrate pattern over *broad areas*, limited only by the sample size. This alignment is due to the spatial match between pattern periodicity  $\lambda$  and the inherent domain scale  $2R$  [defined in Figs. 5(c) and 6(a)], adjusted by the spinning speed of spin-coater.<sup>36</sup>

To fabricate effective electric current paths, the domains of conductive R-P3HT in dielectric polystyrene must be continuous and extend from the free surface throughout the whole film to the substrate. To examine the real distribution of R-P3HT in the PS blend films cast onto silicon wafers patterned with SAM, the 3-dimensional SIMS imaging was applied [Fig. 6(c)]. The SIMS results confirm indeed that the true *lateral (quasi-2-dim)* phase structures are formed.

The novel nonreactive methodology for polymer patterning presented in this article can provide a



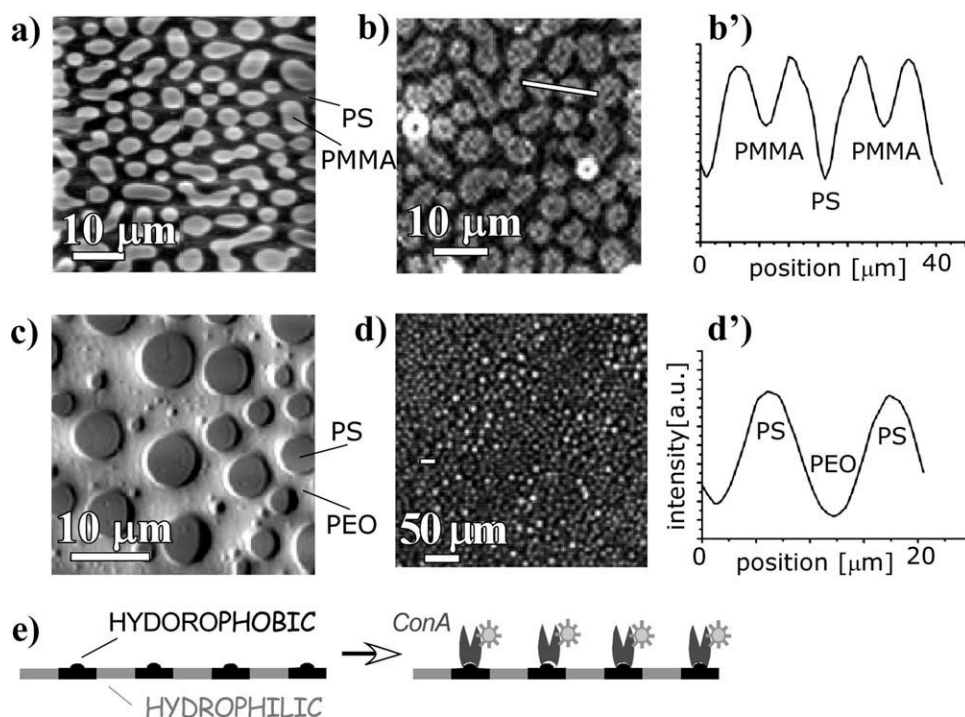


**Figure 7** Selection of polymer pairs for surface patterns that would group proteins. AFM topography<sup>22</sup> (a) and phase contrast (c) images of spin-cast film blends PS:PMMA (a) and PS:PEO (c) and fluorescence micrographs (b,d) and intensity scans (b',d') of adsorbed lectins: lentil lectin LcH (b,b') and concanavalin A ConA (d,d'). Highly selective protein adsorption enabling fabrication of test plates for protein micro-arrays (e) is concluded only for the PS/PEO pair.

simple, solution-processing method to produce polymer-based circuitries, and to integrate them with silicon-based electronics, fabricated on the substrate.

### Polymer patterns grouping proteins

Another interesting problem is the economic fabrication of protein micro-arrays, i.e., proteins grouped in densely packed surface spots smaller than a fraction of millimeter (<250  $\mu\text{m}$ ).<sup>53</sup> A recently studied strategy to fabricate protein micro-arrays is based on the selective protein adsorption to polymer patterns,<sup>8,9,11</sup> for instance, the surface domains of hydrophobic and hydrophilic polymers formed by self-assembly during spin-coating [Fig. 7(e)].<sup>10,22,30,54–60</sup> The patterned proteins, which preserve specific binding with their ligand, can be used to construct tiny counterparts of conventional immunoassays<sup>61</sup> or to induce inhomogeneous cell seeding.<sup>62</sup>

An essential question for this approach is the selection of polymer pairs for the surface patterns that would group selectively adsorbed proteins. Test polymer patterns can be formed by spin-cast polymer blends, with de-mixed blend phases partly wetting the substrate [see Fig. 7(a,c)].<sup>22,29,37</sup> For polymer pairs with small differences in hydrophobicity, such as polystyrene PS and poly(methyl methacrylate) PMMA,<sup>22,30</sup> adsorption of model proteins is

enhanced at polymer (PS/PMMA) interfaces, as indicated by the intensity profile of a cross-section of the fluorescence image [Fig. 7(b')]. This effect, related with the amphipathic character of the proteins and observed also by others,<sup>54,56,57</sup> makes the PS/PMMA pair ill-suited to form patterns grouping the adsorbed proteins. In turn, when the difference in hydrophobicity of the polymers is larger,<sup>22,30</sup> as between polystyrene PS and poly(ethylene oxide) PEO (admixed with PETA and cross-linked with UV light),<sup>22</sup> protein adsorption is highly selective [Fig. 7(c,d,d')], therefore, enabling fabrication of test plates for protein micro-arrays [Fig. 7(e)].

A crucial issue for potential biomedical applications of this approach is preserving the biological activity of proteins adsorbed onto polymer patterns. Such proteins had to still be able to bind specifically with their ligand. As a model protein for the biological activity test, a nonfluorescent glycoprotein carboxypeptidase CaY was used. After selective adsorption of CaY to the PS domains of the PS/PEO pattern [Fig. 8(a)], one-half of the sample was covered by bovine serum albumin BSA [Fig. 8(b)], which is commonly used to block any specific interactions. Then the whole sample was exposed to a solution of fluorescent lectin—concanavalin A (ConA), which specifically recognizes the glycoprotein CaY. The resulting fluorescence micrograph [Fig. 8(d)]

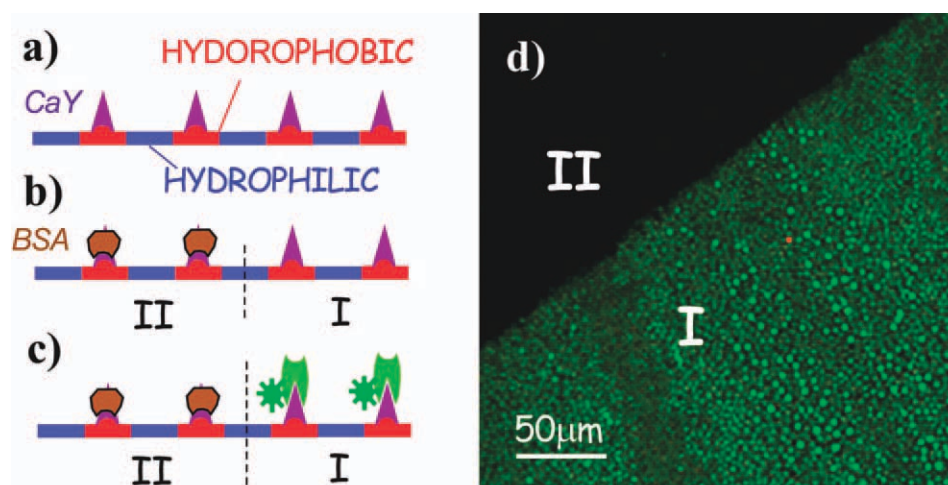


**Figure 8** Biological activity test for model proteins (nonfluorescent CaY), adsorbed selectively to (the PS domains of PS:PEO) polymer (blend) pattern (a), and specifically recognized (region I) by fluorescent lectins ConA (c) visualized on fluorescence micrograph (d).<sup>22</sup> Note that lectins do not bind to the areas (region II) covered by BSA (b) blocking specific interactions. [Color figure can be viewed in the online issue, which is available at [wileyonlinelibrary.com](http://wileyonlinelibrary.com).]

shows ConA present only in the areas (region I) not covered by BSA [Fig. 8(c)]. In addition, the domains of fluorescent ConA reproduce the CaY distribution

guided by the polymer pattern [cf. Figs. 7(c,d) and 8(d)]. This confirms positive result of the biological activity test performed for adsorbed proteins, motivating further studies on the self-assembly of regular polymer blend patterns grouping proteins.

Another challenge is the formation of the microarrays of multiple proteins with the approach using polymer blend patterns grouping biomolecules. Micrometer test plates for multiprotein immunoassays have been fabricated so far mainly with soft lithography.<sup>63–65</sup> The authors propose to apply instead a multi-step selective protein adsorption to the surface domains of hydrophobic and thermoresponsive polymers. This idea is illustrated in Figure 9 with the results obtained for polymer surface patterns formed by spin-cast blends of polystyrene PS and poly(*N*-isopropylacrylamide) PNIPAM. The surface domains rich in PNIPAM and PS form the isolated islands and continuous matrix, respectively. Primary adsorption of model protein (concanavalin ConA labeled with FITC—a green fluorescence marker), performed at 24°C, i.e., below the lower critical solution temperature LCST of PNIPAM in water, resulted in proteins immobilized on the PS-rich hydrophobic domains [Fig. 9(c')]. In turn, secondary adsorption of another model protein (lentil lectin LcH labeled with TRICT—a red fluorescence marker), performed at temperature (38°C) above LCST, yielded effective immobilization of the second protein on the surface domains of PNIPAM (Fig. 9(e')).

## CONCLUSION

The results presented above indicate that the domains self-assembled in the spin-cast polymer

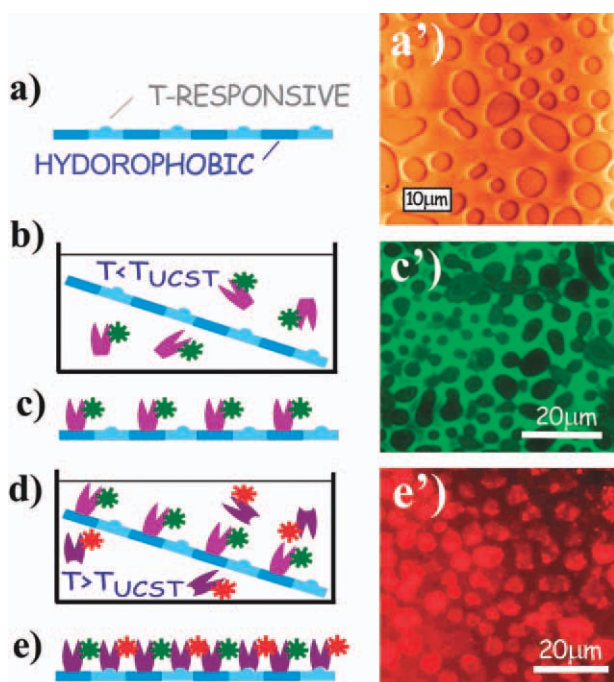


**Figure 9** Micro-arrays of multiple proteins: concanavalin ConA (labeled with FITC) and lentil lectin LcH (labeled with TRICT), visible in fluorescence micrographs (c') and (e'), respectively, formed due to multi-step selective protein adsorption (b,d) to spin-cast blends of thermoresponsive poly(*N*-isopropylacrylamide) PNIPAM and hydrophobic polystyrene PS (a), forming polymer surface patterns (islands of PNIPAM in PS-rich matrix) visible in AFM image (a'). [Color figure can be viewed in the online issue, which is available at [wileyonlinelibrary.com](http://wileyonlinelibrary.com).]



mixtures can form complementary structural elements for electronic and biotechnological devices. However, much work is ahead to make these structural elements technologically useful (e.g., to fabricate efficient solar cells or circuitries, and to produce regular protein patterns). One-step deposition of two blend components with contrasting functionality is merely a first step toward multi-component devices self-assembled in a single process, possibly using specific or multiple interactions between different functional molecules.

The research described in this publication was partly carried out with the equipment (TOF SIMS 5, AFM Agilent 5500) purchased thanks to the financial support of the European Regional Development Fund in the framework of the Polish Innovation Economy Operational Program (contract No.POIG.02.01.00-12-023/08).

## References

1. Leclere, Ph.; Surin, M.; Brocorens, P.; Cavallini, M.; Biscarini, F.; Lazzaroni, R. *Mater Sci Eng* 2006, R55, 1.
2. Forrest, S. R. *Nature* 2004, 428, 911.
3. Tessler, N. *Adv Mater* 1999, 11, 363.
4. McGehee, M. D.; Heeger, A. J. *Adv Mater* 2000, 12, 1655.
5. Friend, R. H.; Gymer, R. W.; Holmes, A. B.; Burroughes, J. H.; Marks, R. N.; Taliani, C.; Bradley, D. D. C.; Dos Santos, D. A.; Brédas, J. L.; Lögdlund, M.; Salaneck, W. R. *Nature* 1999, 397, 121.
6. Brabec, C. J.; Sariciftci, N. S.; Hummelen, J. C. *Adv Funct Mater* 2001, 11, 15.
7. Sirringhaus, H.; Kawase, T.; Friend, R. H.; Shimoda, T.; Inbasekaran, M.; Wu, W.; Woo, E. P. *Science* 2000, 290, 2123.
8. Hong, Y.; Krsko, P.; Libera, M. *Langmuir* 2004, 20, 1123.
9. Suh, K. Y.; Song, J.; Khademhosseini, A.; Laibinis, P. E.; Tager, R. *Biomaterials* 2004, 25, 557.
10. Kumar, N.; Halm, J. *Langmuir* 2005, 21, 6652.
11. Petrou, P. S.; Chatzichristidi, M.; Douvas, A. M.; Argitis, P.; Misiakos, K.; Kakabakos, S. E. *Biosens Bioelectron* 2007, 22, 1994.
12. Lawrence, C. J. *Phys Fluids* 1988, 31, 2786.
13. Bao, Z.; Feng, Y.; Dodabalapur, A.; Raju, V. R.; Lovinger, A. J. *Chem Mater* 1997, 9, 1299.
14. Granlund, T.; Nyberg, T.; Roman, L. S.; Svensson, M.; Inganäs, O. *Adv Mater* 2000, 12, 269.
15. Berggren, M.; Inganäs, O.; Gustafsson, G.; Rasmusson, J.; Andersson, M. R.; Hjertberg, T.; Wennerström, O. *Nature* 1994, 372, 444.
16. Halls, J. M.; Walsh, C. A.; Greenham, N. C.; Marsegila, E. A.; Friend, R. H.; Moratti, S. C.; Holmes, A. B. *Nature* 1995, 376, 498.
17. Moons, E. *J Phys Condens Mater* 2002, 14, 12235.
18. Chua, L.-L.; Ho, P. K. H.; Sirringhaus, H.; Friend, R. H. *Adv Mater* 2004, 16, 1609.
19. Corcoran, N.; Arias, A. C.; Kim, J. S.; MacKenzie, J. D.; Friend, R. H. *Appl Phys Lett* 2003, 82, 299.
20. Björström-Svanström, C. M.; Rysz, J.; Bernasik, A.; Budkowski, A.; Zhang, F.; Inganäs, O.; Andersson, M. R.; Magnusson, K. O.; Benson-Smith, J. J.; Nelson, J.; Moons, E. *Adv Mater* 2009, 21, 4398.
21. Jaczewska, J.; Budkowski, A.; Bernasik, A.; Raptis, I.; Moons, E.; Goustouridis, D.; Haberko, J.; Rysz, J. *Soft Mater* 2009, 5, 234.
22. Zemła, J.; Lekka, M.; Raczowska, J.; Bernasik, A.; Rysz, J.; Budkowski, A. *Biomacromolecules* 2009, 10, 2101.
23. Björström, C. M.; Bernasik, A.; Rysz, J.; Budkowski, A.; Nilsson, S.; Svensson, M.; Andersson, M. R.; Magnusson, K. O.; Moons, E. *J Phys Condens Mater* 2005, 17, L529.
24. Björström, C. M.; Nilsson, S.; Magnusson, K. O.; Moons, E.; Bernasik, A.; Rysz, J.; Budkowski, A.; Zhang, F.; Inganäs, O.; Andersson, M. R. *Proc SPIE* 2006, 6192, X1921.
25. Björström, C. M.; Nilsson, S.; Bernasik, A.; Budkowski, A.; Magnusson, K. O.; Moons, E. *Appl Surf Sci* 2007, 253, 3906.
26. Nilsson, S.; Bernasik, A.; Budkowski, A.; Moons, E. *Macromolecules* 2007, 40, 8291.
27. Jaczewska, J.; Budkowski, A.; Bernasik, A.; Raptis, I.; Raczowska, J.; Goustouridis, D.; Rysz, J.; Sanopoulou, M. *J Appl Polym Sci* 2007, 105, 67.
28. Jaczewska, J.; Raptis, I.; Budkowski, A.; Goustouridis, D.; Raczowska, J.; Sanopoulou, M.; Pamuła, E.; Bernasik, A.; Rysz, J. *Syn Metals* 2007, 157, 726.
29. Jaczewska, J.; Budkowski, A.; Bernasik, A.; Moons, E.; Rysz, J. *Macromolecules* 2008, 41, 4802.
30. Zemła, J.; Lekka, M.; Wiltowska-Zuber, J.; Budkowski, A.; Rysz, J.; Raczowska, J. *Langmuir* 2008, 24, 10253.
31. Budkowski, A.; Bernasik, A.; Moons, E.; Lekka, M.; Zemła, J.; Jaczewska, J.; Haberko, J.; Raczowska, J.; Rysz, J.; Awskiuk, K. *Acta Phys Pol A* 2009, 115, 435.
32. Jones, R. A. L.; Norton, L. J.; Kramer, E. J.; Bates, F. S.; Wiltzius, P. *Phys Rev Lett* 1991, 66, 1326.
33. Binder, K. *Adv Polym Sci* 1999, 138, 1.
34. Geoghegan, M.; Krausch, G. *Prog Polym Sci* 2003, 28, 261.
35. Böltau, M.; Walheim, S.; Mlynek, J.; Krausch, G.; Steiner, U. *Nature* 1998, 391, 877.
36. Raczowska, J.; Cyganik, P.; Budkowski, A.; Bernasik, A.; Rysz, J.; Raptis, I.; Czuba, P.; Kowalski, K. *Macromolecules* 2005, 38, 8486.
37. Budkowski, A. *Adv Polym Sci* 1999, 148, 1.
38. Heriot, S. Y.; Jones, R. A. L. *Nat Mater* 2005, 4, 782.
39. Spanggaard, H.; Krebs, F. C. *Solar Energy Mater Solar Cells* 2004, 83, 125.
40. Hoppe, H.; Sariciftci, N. S. *J Mater Chem* 2006, 14, 45.
41. Chen, L.-M.; Xu, Zh.; Hong, Z.; Yang, Y. *J Mater Chem* 2010, 20, 2575.
42. Halls, J. J. M.; Pichler, K.; Friend, R. H.; Moratti, S. C.; Holmes, A. B. *Appl Phys Lett* 1996, 68, 3120.
43. Treat, N. D.; Brady, M. A.; Smith, G.; Toney, M. F.; Kramer, E. J.; Hawker, C. J.; Chabiny, M. L. *Adv Energy Mater* 2011, 1, 82.
44. Salleo, A. *Mater Today* 2007, 10, 38.
45. Arias, A. C.; Endicott, F.; Street, R. A. *Adv Mater* 2006, 18, 2900.
46. Qiu, L.; Lim, J. A.; Wang, X.; Lee, W. H.; Hwang, M.; Cho, K. *Adv Mater* 2008, 20, 1141.
47. Granström, M.; Berggren, M.; Pedo, D.; Inganäs, O.; Andersson, M. R.; Hjertberg, T.; Wennerström, O. *Supramol Sci* 1997, 4, 27.
48. Granström, M.; Inganäs, O. *Appl Phys Lett* 1996, 68, 147.
49. Rysz, J.; Budkowski, A.; Bernasik, A.; Klein, J.; Kowalski, K.; Jedlinski, J.; Fetters, L. J. *Europhys Lett* 2000, 50, 35.
50. Coffey, D. C.; Ginger, D. S. *J Am Chem Soc* 2005, 127, 4565.
51. Wei, J. H.; Coffey, D. C.; Ginger, D. S. *J Phys Chem B* 2006, 110, 24324.
52. Salleo, A.; Arias, A. C. *Adv Mater* 2007, 19, 3540.
53. Angedent, P. *DDT* 2005, 10, 503.
54. Morin, C.; Hitchcock, A. P.; Cornelius, R. M.; Brash, J. L.; Urquhart, S. G.; Scholl, A.; Doran, A. *J Electron Spectrosc Relat Phenomena* 2004, 137-140, 785.
55. Sousa, A.; Sengonul, M.; Latour, R.; Kohn, J.; Libera, M. *Langmuir* 2006, 22, 6286.

56. Li, L.; Hitchcock, A. P.; Robar, N.; Cornelius, R.; Brash, J. L.; Scholl, A.; Doran, A. *J Phys Chem B* 2006, 110, 16763.
57. Li, L.; Hitchcock, A. P.; Cornelius, R.; Brash, J. L.; Scholl, A.; Doran, A. *J Phys Chem B* 2008, 112, 2150.
58. Leung, B. O.; Wang, J.; Brash, J. L.; Hitchcock, A. P. *Langmuir* 2009, 25, 13332.
59. Wan, L. S.; Ke, B. B.; Meng, X. L.; Zhang, L. Y.; Xu, Z. K. *Sci China Ser B Chem* 2009, 52, 969.
60. Aaron Kau, K. H.; Bang, J.; Kim, D. H.; Knoll, W. *Adv Funct Mater* 2008, 18, 3148.
61. Zhu, H.; Snyder, M. *Curr Opin Chem Biol* 2003, 7, 55.
62. Persen, D.; Haviland, D. B. *ACS Appl Mater Interfaces* 2009, 3, 543.
63. Bernard, A.; Renault, J. P.; Michel, B.; Bosshard, H. R.; Delamar, E. *Adv Mater* 2000, 12, 1067.
64. Inerowicz, H. D.; Howell, S.; Regnier, F. E.; Reifenberger, R. *Langmuir* 2002, 18, 5263.
65. Chalmeau, J.; Thibault, C.; Carcenac, F.; Vieu, C. *Appl Phys Lett* 2008, 93, 133901.